ISSN NO: 2770-4491
Date of Publication:20-08-2022

Mixed Convection Heat Transfer of Al_2O_3-H_2O Nanofluid in a Trapezoidal Lid-driven Cavity at Different Angles of Inclination

Akeel Abdullah Mohammed [a] , Maria Thaer [a] , Duaa Qays Yahya [b]
[a] Al-Nahrain University/ College of Engineering, Mechanical Engineering Department
[b] University of Baghdad/ College of Engineering
st.mariya.th.abdulhadi@ced.nahrainuniv.edu.iq

Abstract: Mixed convection in a trapezoidal lid driven cavity containing a heat source circular cylinder using two fluids separately: H_2O base fluid and H_2O-Al_2O_3 nanofluids has been investigated numerically using Ansys commercial program (ANSYS Fluent 2021 R2). The small horizontal wall is moved at constant velocity, while the other parallel large wall is stationary. Both walls are cold while the other inclined walls of cavity are insulated adiabatically. Validation the present work is achieved and a comparison with the beforehand published work is performed and found to be in excellent agreement with average difference about 1.52 %. The results cover three values of Richardson number (Ri=0.01, 1, and 10), two values of radius ratio (RR=0.2 and 0.25), four positions of the inner cylinder (middle, right, top, bottom), and four angles of inclination ($\varphi = 0^o$, 45^o, 90^o, and 180^o). It is noticed that, for the angles ($\varphi = 0^o$, 45^o, and 90^o); the bottom position $(0, -0.15)$ is the best position giving the highest value of average Nusselt number. While, the higher heat transfer rate is produced for ($\varphi = 180^o$) at top position $(0, 0.15)$.

Key words: mixed convection, triangular cavity, lid-driven, adiabatic body.

1. Introduction

Mixed convection heat transfer occurs also in enclosures with moving upper wall, lower wall, or both walls. Lid-driven enclosures with different geometries, boundary conditions, and enhancement techniques has received great attention by authors because of its importance in the industrial applications. Examples of applications can be found in nuclear reactors, cooling of electronic equipment's, solar energy, and technology of lubrication [1]. Different heat transfer enhancement techniques were used to investigate the problem of mixed convection in lid-driven cavities. Increasing the thermal conductivity of the base fluid by using nanofluids [1-15], and porous medium [16-21] is one of the effective of these techniques. Other methods include applying the magnetic field or vibration on the cavity in one direction or more with or without nanofluids [22-32].

The present work is a numerical study for the mixed convection heat transfer in a lid-driven inclined trapezoidal cavity filled with a H_2O-Al_2O_3 nanofluid using Ansys commercial program (ANSYS Fluent 2021 R2). The heat source consists of a circular cylinder heated isothermally at T_h. The moving upper wall and the stationary bottom wall are cooled isothermally at T_c. The inclined walls of cavity are adiabatically insulated. The top wall moves at constant velocity, while the other walls are stationary. The Richardson numbers considered in this study are 0.01, 1, and 10. Four positions of inner cylinder inside cavity have been taken in consideration (top, bottom, middle, middle right side). Two values of radius ratio (RR=0.2 and 0.25), four nanoparticles volume fractions ($\phi = 0, 0.04, 0.06, and\ 0.08$) and four angles of cavity inclination (0^o, 45^o, 90^o, and 180^o) have been choice in the present work.

2. Mathematical Model

2.1. Physical Domain and assumptions

Two-dimensional, steady, and laminar mixed convection heat transfer inside trapezoidal cavity is studied numerically. The working fluid is assumed to be incompressible and Newtonian. The Boussinesq's approximation is chosen to describe the variation of temperature as a function of density and to couple in this way the temperature field to the flow field. The dissipation effect due to the viscous term is neglected. No heat generation is considered.

ISSN NO: 2770-4491
Date of Publication:20-08-2022

The physical domain of a trapezoidal lid-driven, for cases taken in the present study, is schematically shown in Fig. 3.1. The cavity consists of two parallel cold walls with constant temperature T_c. The top short wall is moving at constant velocity in the positive x-direction. While, the inclined walls are insulated adiabatically. The inner cylinder is heated isothermally at T_h. Two values of radius of inner cylinder r_o are taken in this study to give two radius ratios. The cavity is inclined at an angle φ with the horizontal reference x-axis and thus arising opposing flow condition where the shear flow caused by the moving top wall opposes the buoyancy driven flow caused by the thermal non-homogeneity of the cavity boundaries.

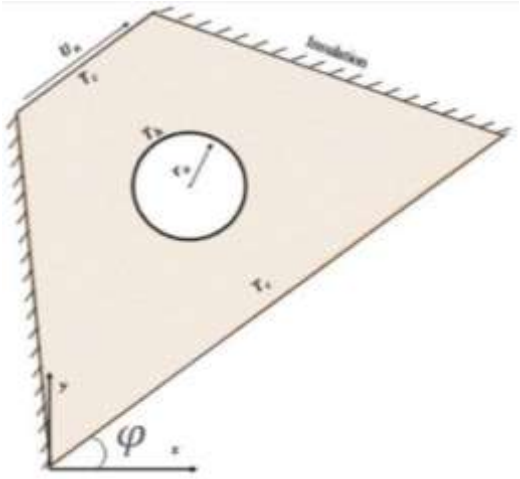

Figure 1: Physical model.

2.2. Governing Equations and Boundary Conditions

The conservation of mass, momentum and energy equations in the dimensionless form as follows [33]:

$$\frac{\partial U}{\partial X}+\frac{\partial V}{\partial Y}=0, \tag{1}$$

$$U\frac{\partial U}{\partial X}+V\frac{\partial U}{\partial Y}=-\frac{\partial P}{\partial X}+\frac{1}{Re}\frac{\mu_{eff}}{\vartheta_f\rho_{eff}}\left[\frac{\partial^2 U}{\partial X^2}+\frac{\partial^2 U}{\partial Y^2}\right]+\frac{(\rho\beta)_{eff}}{\rho_{eff}\beta_f}.(Ri\ sin\varphi)\theta, \tag{2}$$

$$U\frac{\partial V}{\partial X}+V\frac{\partial V}{\partial Y}=-\frac{\partial P}{\partial Y}+\frac{1}{Re}\frac{\mu_{eff}}{\rho_{eff}\,\vartheta_f}\left[\frac{\partial^2 V}{\partial X^2}+\frac{\partial^2 V}{\partial Y^2}\right]+\frac{(\rho\beta)_{eff}}{\rho_{eff}\beta_f}(Ri\ cos\varphi)\theta, \tag{3}$$

$$U\frac{\partial \theta}{\partial X}+V\frac{\partial \theta}{\partial Y}=\frac{1}{Re\,Pr}\frac{\alpha_{eff}}{\alpha_f}\left[\frac{\partial^2 \theta}{\partial X^2}+\frac{\partial^2 \theta}{\partial Y^2}\right], \tag{4}$$

The dimensionless variables. can be written as follows:

$$U=\frac{u}{U_o},\quad V=\frac{v}{U_o},\quad X=\frac{x}{L},\quad Y=\frac{y}{L},\quad \theta=\frac{T-T_c}{T_h-T_c},\quad P=\frac{p}{\rho_{eff}U_o^2}, \tag{5}$$

$$Re=\frac{U_o\,L}{\vartheta_f},\quad Pr=\frac{\vartheta_f}{\alpha_f},\quad Gr=\frac{g\beta L^3(T_h-T_c)}{\vartheta_f^2},\quad Ri=\frac{Gr}{Re^2}, \tag{6}$$

The boundary conditions in dimensionless form are presented in **Table 1.** The symbol $'n'$ represents the normal direction on the inclined walls.

Table 1 boundary conditions

	U	V	Θ
Top wall	A=1	0	0
Bottom wall	0	0	0
Left and right walls:	0	0	$\frac{\partial\theta}{\partial n}=0$
Inner cylinder wall	0	0	1

ISSN NO: 2770-4491
Date of Publication:20-08-2022

2.3. Thermophysical Properties of the Working Fluids

The general equations for effective thermophysical properties fluently were developed and implemented as follows [6].

$$\rho_{eff} = (1-\phi_p)\rho_f + \phi_p\rho_s\,, \quad (7)$$

$$\mu_{eff} = (1.125 - 0.0007 \times T)\mu_f, \quad (8)$$

$$\phi_p = 1\% \quad 20 \le T[℃] \le 70,$$

$$\mu_{eff} = (2.1275 - 0.0215 \times T + 0.0002 \times T^2)\mu_f, \quad (9)$$

$$\phi_p = 4\% \quad 20 \le T[℃] \le 70,$$

$$\frac{k_{eff}}{k_f} = 1.0 + 1.0112\phi_p + 2.437\phi_p\left(\frac{47}{d_p(nm)}\right) - 0.0248\phi_p\left(\frac{k_p}{0.613}\right), \quad (10)$$

$$\beta_{eff} = \left(-0.479\phi_p + 9.3158 \times 10^{-3}T - \frac{4.7211}{T^2}\right) \times 10^{-3} \quad (11)$$

$$0 \le \phi_p \le 0.04 \quad 10 \le T[℃] \le 40,$$

$$c_{eff} = \frac{(1-\phi_p)\rho_f c_f + \phi_p\rho_{sp}c_p}{\rho_{eff}}\,, \quad (12)$$

Table 1 Thermophysical properties of the water, Al_2O_3 nanoparticles and H_2O-Al_2O_3 nanofluid [13].

Material	$C_p\ (J/kg.K)$	$\rho\ (kg/m^3)$	$k\ (W/m.K$	$\beta\ (1/K)$	$\mu(Pa.s)$
H_2O	4179	997.1	0.613	21×10^{-5}	0.001003
Al_2O_2	765	3970	40	0.85×10^{-5}	-
H_2O-Al_2O_3 ($\Phi = 8\ \%$)	3547.8	1135.68	0.9552	-	0.0012036
H_2O-Al_2O_3 ($\Phi = 6\ \%$)	3691.5	1101.26	0.8664	-	0.00115345
H_2O-Al_2O_3 ($\Phi = 2\ \%$)	4007.6	1032.42	0.6888	-	0.00105315

2.2 Boundary conditions

The boundary conditions in dimensionless form are presented in Table 2. The symbol 'n' represents the normal direction on the inclined walls.

Table 2 *Boundary* conditions.

	U	***V***	**Θ**
Top wall	A=1	0	0
Bottom wall	0	0	0
Left and right walls:	0	0	$\frac{\partial\theta}{\partial n} = 0$
Inner cylinder wall	0	0	1

2.3. Thermophysical Properties of Nanofluid

The general equations for effective thermophysical properties fluently were developed and implemented as follows [34].

$$\rho_{eff} = (1-\phi_p)\rho_f + \phi_p\rho_s\,, \quad (7)$$

$$\mu_{eff} = (1.125 - 0.0007 \times T)\mu_f, \quad (8)$$

$$\phi_p = 1\% \quad 20 \le T[℃] \le 70,$$

$$\mu_{eff} = (2.1275 - 0.0215 \times T + 0.0002 \times T^2)\mu_f, \quad (9)$$

$$\phi_p = 4\% \quad 20 \le T[℃] \le 70,$$

$$\frac{k_{eff}}{k_f} = 1.0 + 1.0112\phi_p + 2.437\phi_p\left(\frac{47}{d_p(nm)}\right) - 0.0248\phi_p\left(\frac{k_p}{0.613}\right) \quad (10)$$

ISSN NO: 2770-4491
Date of Publication:20-08-2022

$$\beta_{eff} = \left(-0.479\phi_p + 9.3158 \times 10^{-3}T - \frac{4.7211}{T^2}\right) \times 10^{-3} \quad (11)$$

$0 \le \phi_p \le 0.04 \quad 10 \le T[℃] \le 40,$

$$c_{eff} = \frac{(1-\phi_p)\rho_f c_f + \phi_p \rho_{sp} c_p}{\rho_{eff}}, \quad (12)$$

The thermophysical properties of the base fluid, nanoparticle, and nanofluid are presented in Table 3. The nanofluids being used correspond to a mixture of water (base fluid) with aluminum oxide. The required properties of this problem include density, heat capacity, effective thermal conductivity, effective dynamic viscosity and thermal expansion.

Table 3 Thermophysical properties of the water, Al_2O_3 nanoparticles and H_2O-Al_2O_3 nanofluid [34]..

Material	$C_p\ (J/kg.K)$	$\rho\ (kg/m^3)$	$k\ (W/m.K)$	$\beta\ (1/K)$	$\mu(Pa.s)$
H_2O	4179	997.1	0.613	21×10^{-5}	0.001003
Al_2O_2	765	3970	40	0.85×10^{-5}	-
H_2O-Al_2O_3 ($\Phi = 8\ \%$)	3547.8	1135.68	0.9552		0.0012036
H_2O-Al_2O_3 ($\Phi = 6\ \%$)	3691.5	1101.26	0.8664		0.00115345
H_2O-Al_2O_3 ($\Phi = 2\ \%$)	4007.6	1032.42	0.6888		0.00105315

2.4. Geometry and Mesh Generation

The mesh computational generation is a suitable for solving the two-dimensional conservation of complicated geometries for energy equation, continuity equation, and momentum equation. The volume meshing mainly has two approaching types, the structured meshing and unstructured meshing. The governing equations in the structured mesh are transformed in the curvilinear coordinate system aligned with the surface. But for the complex geometries, the mesh generation is required for time consuming and mostly requires modifications on model's geometry. So, it is good choice for simple shapes. However, it becomes too inefficient and requires a long time for complex geometries. Therefore, it has been excluded in this research. Unstructured grids are in general more suitable for complex geometries, so it is used in the present work. In present study, the discretization grid is triangular, unstructured and non-uniform as shown in **Figure 2**.

2.5. Grid Independence Test

A grid independence test was carried out to obtain the most suitable mesh face number and size for this particular geometry. In this study, five element sizes are considered,1, 0.8, 0.6, 0.4, 0.2 at RR=0.2 and $Re = 100$. Given that the discretization grid is triangular, unstructured and non-uniform. **Figure 3** shows the variation Nusselt number for different element sizes. It is seen that; the element size of 0.2 gives almost identical results for the Nusselt number. Ultimately, a mesh number of 56400 was used in this study as this represented the best compromise in terms of both accuracy and computational time.

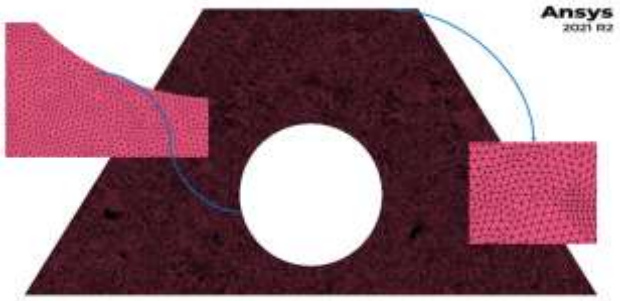

Figure 2: Mesh generation.

ISSN NO: 2770-4491
Date of Publication:20-08-2022

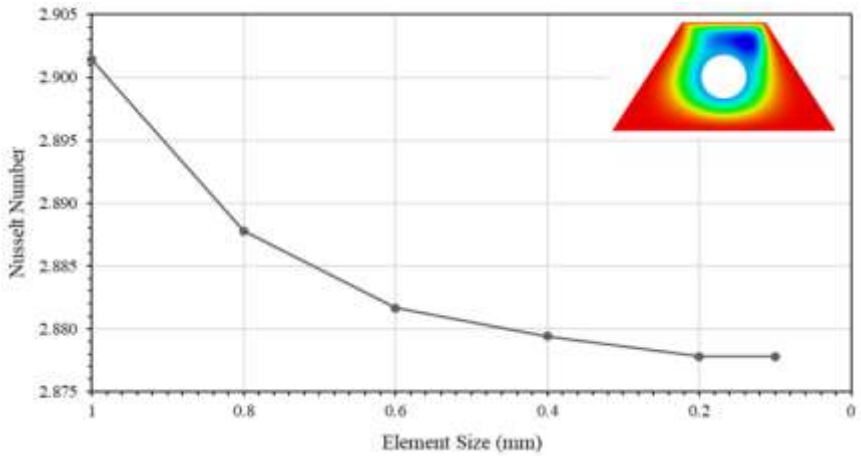

Figure 3: Convergence of the average Nusselt number with Element size.

2.4 Numerical Solution

The solution methods can specify various parameters associated with the solution method to be used in the calculation. The governing equations subject to considered boundary conditions are solved by using Ansys commercial program (ANSYS Fluent 2021 R2). Firstly, grid is generated, and ANSYS Fluent uses the solution algorithm to solve the governing equations sequentially by using (SIMPLE) scheme. In addition, spatial discretization of pressure, momentum, turbulent kinetic energy, and the turbulent dissipation rate were second order upwind. SIMPLE is an acronym for Semi-Implicit Method for Pressure-Linked Equations. It is a numerical procedure that generally sees use in solving the Navier-Stokes equations. The local Nusselt number based on the length of the top wall of trapezoidal cavity is written as:

$$Nu_L = \frac{k_{eff}}{k_f}\frac{\partial\theta}{\partial Y}\Big|_{Y=1} \qquad (14)$$

The average Nusselt number of the hot cylinder lid-driven wall is given as follows:

$$Nu_m = \int_0^1 Nu_L(X)\,dX \qquad (15)$$

3. Validation

The present simulation method has been validated with streamlines and isotherms results of Khanafer et al. [35] works. The comparison includes the values of average Nusselt numbers for both studies as shown in Table (3). This work analyzed the mixed convection air flow inside square cavity heated from the bottom wall and having inner circular cylinder with radius ratio (radius of cylinder to length of one wall) of 0.2. The working fluid was the air (Pr=0.7). Four values of Richardson number (0.01, 1, 5, and 10) were choice for validation. The validation results the values of average Nusselt number for both simulations are close to each other with average difference 1.5%.

Table 3 Nusselt number values for validation the present work with Khanafer et al. work's [35]

Ri	$Nu_{previous}$[35]	$Nu_{current}$	$difference$
0.01	2.93	2.98	1.7%
1	3.5	3.6	2.8%
5	4.7	4.77	1.4%
10	5.06	5.09	0.19%

4. Results And Discussion

4.1 Streamlines and isotherms

The effect of Richardson number on streamlines and isotherms inside lid-driven cavity with nanoparticles volume fraction ($\phi = 0.08$) and four angles of inclination ($\varphi = 0^o$, 45^o, 90^o, and 180^o) is shown in **Figure 4**; respectively. Generally, the behavior of streamlines and isotherms depends strongly on

ISSN NO: 2770-4491
Date of Publication:20-08-2022

Richardson numbers, volume fractions, and angles of inclination. The value of the Richardson number, $Ri=Gr/Re^2$ indicates the importance of buoyancy driven free convection (secondary flow) relative to the lid driven forced convection (primary flow).

It is clear from Figure that, for $\varphi = 0^o$ (top moving wall) and Ri=0.01 that there is main vortex having center located in the top right side of cavity. This vortex rotates clockwise in the same of motion direction. It extends towards the right bottom side and seems to be stronger as Richrdson number increases to 1 and 10 because increasing the effects of secondary flow due to high natural convection. Generally, the moving wall helps to motion the fluid in the same direction, then the fluid collides with the nearest wall to change its motion towards the opposite direction, causing a rotational motion (vortex).

For Ri=0.01 (the Buoyancy effects are small), the high gross flow generated by the movement of the top wall causes the main circulation fills the entire cavity. It is evident that the shear influences due to moving the top wall is prevalent for all angles of inclination. So, the isotherms indicated that the hydrodynamic and thermal boundary layers are not developed. The isothermal lines are mostly undistorted and parallel to the thermal plum. In the large recirculation zone temperature gradients are very weak because of the well mixed of liquid resulted from the strong action of the mechanically driven circulations. As a result, the temperature differences in the enclosure region are very small. With increase in Richardson number, the temperatures increase and the isotherms far away from hot cylinder towards the cold walls. The thermal plum is getting stronger with increase in Richardson number. Its direction depends strongly on the angle of inclination, type of fluid (with and without adding of nanoparticles), and Richardson number. Increasing Richardson number to one means the process is mixed convection and the inertia force and the buoyancy force are equivalent. There are two flows in this case: aiding flow and opposing flow. Where the direction of primary flow is the same as the direction of buoyancy force (towards down), the flow is called aiding. While, when the inertia force direction (primary flow) is upwards (i.e., opposite the buoyancy force), the process is called opposing. In the present study, the flow is aiding.

The figure 4 shows that for $\varphi = 45^o$ (inclined moving wall), the main vortex extends above the cylinder in parallel with the moving wall for Ri=1. This means the maximum stream function is weaker than that in the case of dominant forced convection Ri=0.01. The strength of vortex increases as the primary flow increases (i.e., increasing the speed of moving wall and decreasing Richardson number to 0.01) with and without adding nanoparticles into the base fluid. The vortex cleavages into two strong parts in the case of dominant natural convection (Ri=10) due to high natural convection currents.

For $\varphi = 90^o$ (vertical moving wall), the behavior of streamlines is nearly similar to that case of $\varphi = 45^o$. The main vortex cleavages into two weak parts for (Ri=1 with aiding flow. While, the vortex stays strong for Ri=10, because the dominant of natural convection in the heat transfer process. For Ri=0.01, the vortex seems to be stronger than that for Ri=1 and weaker than that for Ri=10. Adding the nanoparticles into the base fluid with high nanoparticles volume fraction for (Ri=10) produces two major vortices and two minor weak vortices.

It is clear that the streamlines inside lid driven cavity with bottom cylinder position for radius ratio =0.25, $\varphi = 180^o$ (bottom moving wall). It is seen that the main vortex lies below the hot cylinder and upper the moving wall at Ri=0.01because of higher shearing action at this region due to dominant forced convection. This vortex extends and becomes stronger with adding nanoparticles $\phi = 0.08$ because the strong effect of primary flow resulted from moving the bottom small wall. The main vortex is divided into three vortices with different strengths if Richrdson increases into one (mixed convection). The maximum stream function occurs at bottom of cavity above the moving wall. Decreasing the primary flow at the expense of the secondary flow in closed cavities gives opposite behavior to the case of open conduit. It is noticed that there are two main strong vortices on either side of lid-driven cavity. It is expected this gives higher heat transfer rate than other values of Richardson number.

When Ri=10, natural convection is stronger than forced convection. The Buoyancy assists the primary flow and thus the convection currents become stronger with increasing Richardson number. As a result, the isothermal lines become more intense near the cold lid. Developing of the hydrodynamic and thermal boundary layers along the cold wall and hot wall will be happened. Additionally, the maximum temperature reduces leading to obtain higher heat transfer rate. It is evident that, the isotherms produced higher temperature gradients in the region adjacent to the hot cylinder walls. The isotherms are rotated about the

ISSN NO: 2770-4491
Date of Publication:20-08-2022

hot circular cylinder with circular lines topped by thermal plum in a small region near the hot wall. Whereas, these lines far away from the hot cylinder wall towards the cold walls because the dominant forced convection. Formation two plums for high Richardson number indicates higher heat transfer rate occurs inside lid-driven cavity with $\varphi = 180^o$ (bottom moving wall). Generally, it is expected that increasing the nanoparticles volume fraction more than (0.1) may reduce the thermal diffusivity of liquid and produces negative effects on the fluid flow and heat transfer inside cavity. These effects are more pronounced for $Ri \geq 1$.

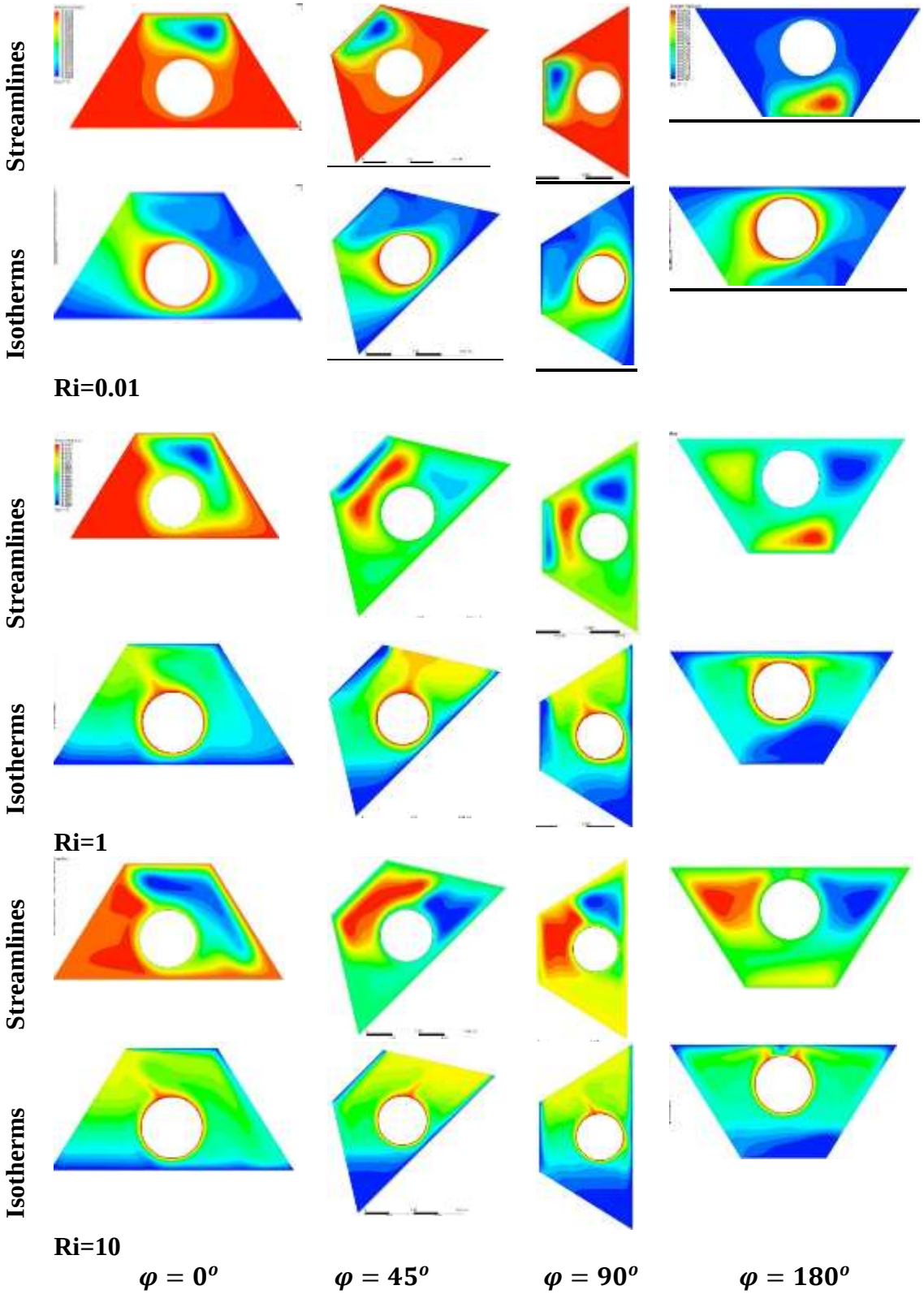

Figure 4 Streamlines and isotherms inside lid driven cavity with bottom cylinder position for radius ratio =0.25, $\phi = 0.08$.

ISSN NO: 2770-4491
Date of Publication:20-08-2022

4.2 Nusselt number

The mean Nusselt number versus nanoparticles volume fraction at different values of Richardson numbers and for angle of cavity inclination ($\varphi = 0^0, 45^0, 90^0, and\ 180^0$) are shown in **Figure 5**; respectively. It is observed that the average Nusselt number for all ranges of volume fraction increases with an increase in the Richardson number. The average Nusselt numbers for $\varphi = 180^0$ (bottom lid-driven) are higher than that for other inclination angles at Ri=10 (dominant natural convection) and nanoparticles volume fraction ϕ=0, 0.02, and 0.06. This behavior is reverse at ϕ=0.08 in which the angle of inclination $\varphi = 0^0$ (top lid-driven) produces the highest value of average Nusselt number than other angles of inclination. As a result, the energy exchange rates in the fluid will be boosted leads to consequently enhancing the thermal dispersion of the flow. For Ri=0.01 (dominant forced convection) and $\varphi = 45^o$ (inclined lid-driven), the mean Nusselt number decreases with increase in ϕ from 0.06 to 0.08. The combined effect of inclined direction of moving wall and the high fraction of nanoparticles cause decrease in heat transfer rate. The same behavior is noticed for Ri=10 (dominant natural convection) and $\varphi = 180^o$ (bottom lid-driven).

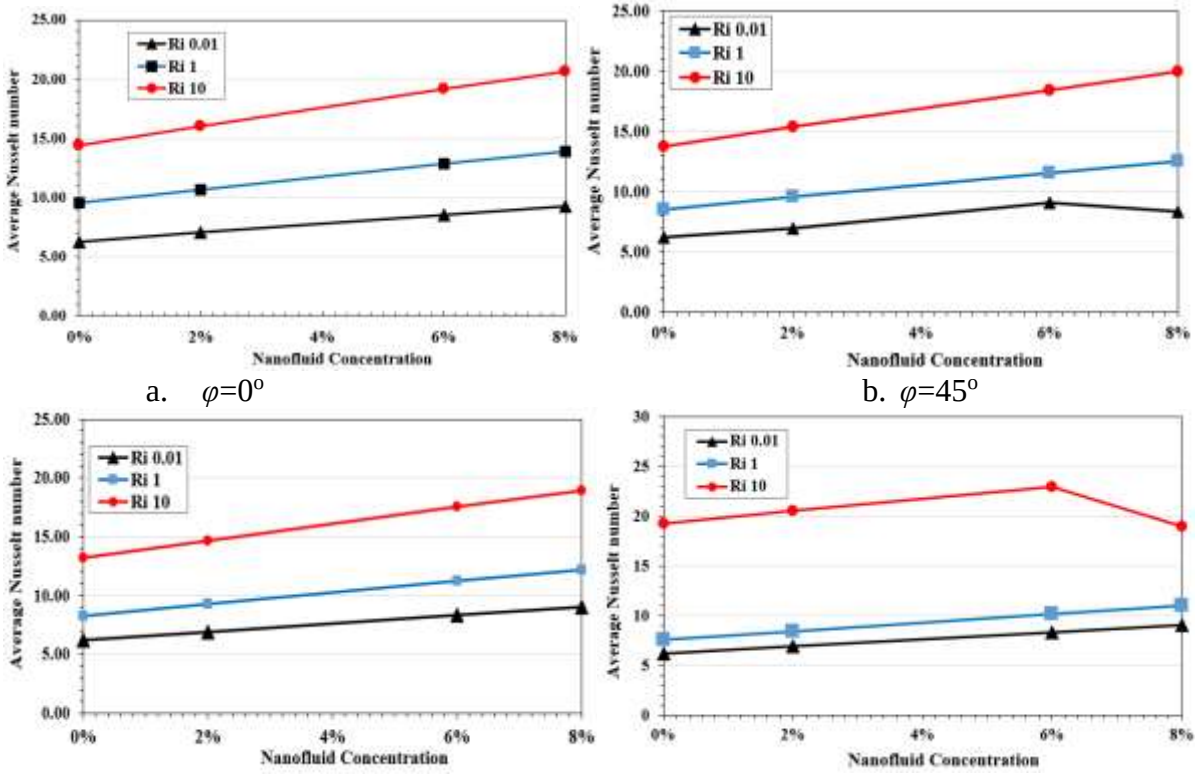

a. φ=0^o b. φ=45^o

c. φ=90^o d. φ=180^o

Figure 5 Average Nusselt number around inner cylinder for Al_2O_3-H_2 O nanofluid with different volume factions of nanoparticles and angles of inclination

5. Conclusions

1. The heat transfer rate increases as Richardson number increases because increasing the free convection currents (secondary flow).
2. Generally, it is obvious that the heat transfer process enhances with increasing of nanoparticles volume fraction.
3. The extension in streamlines for Ri=1 and 10 is more pronounced than that for Ri=0.01, especially at $\varphi = 0^o$and 180^o.
4. The maximum values of maximum stream function occur for Ri=10 (i.e., dominating natural convection) for all angles of inclinations and volume fractions of nanoparticles.
5. Decreasing the primary flow at the expense of the secondary flow in closed cavities gives opposite behavior to the case of open conduit.

ISSN NO: 2770-4491
Date of Publication:20-08-2022

6. It is noticed that the thermal plum moves towards clockwise on the hot cylinder as Richardson number increases from 0.01 to 1.
7. Generally, the angle of inclination $\varphi = 180^o$ (bottom moving wall) produces the lowest local Nusselt numbers than other angles for Ri=0.01 and 1.
8. The average Nusselt numbers for $\varphi = 180^0$ (bottom lid-driven) are higher than that for other inclination angles at Ri=10 and nanoparticles volume fraction ϕ=0, 0.02, and 0.06. This behavior is reverse at ϕ=0.08 in which the angle of inclination $\varphi = 0^0$ (top lid-driven) produces the highest value of average Nusselt number than other angles of inclination.

Abbreviations

Al_2O_3 = aluminium oxide
CuO =copper oxide
CFD =Computational Fluid Dynamics
Gr =Grashof number (gβmΔTW3 /νm 2)
Da =Darcy number
h = convective heat transfer coefficient (W/m2K)
Nu = Nusselt number
Pr = Prandtl number (νm/αm)
Ra = Rayleigh number (Gr * Pr)
Re = Reynolds number (Uo*W/ν)
Ri =Richardson number (Gr/Re2)
RR =A aspect ratio
r_0 = radius of inner cylinder
U =dimensionless velocity component at x-direction
u =velocity component at x-direction (m/s)
U0 = lid velocity (m/s)

Greek symbols:

α =thermal diffusivity of the fluid (m2 /s)
α =under-relaxation factor
β = volumetric coefficient of thermal expansion (1/K)
μ =dynamic viscosity of the fluid (Pa/s)
ν = kinematic viscosity of the fluid (m2 /s)
φ =volume fraction of nanoparticles
φ =inclined at an angle
ψ max =Maximum stream function γ = azimuth angle

Subscripts:

Tc =constant temperature Th =hot temperature
nf =Nano fluid np =nanoparticles

References

1. Zoubair Boulahia, Abderrahim Wakif, and Rachid Sehaqui. Mixed convection heat transfer of Cu-water nanofluid in a lid driven square cavity with several heated triangular cylinders. International Journal of Innovation and Applied Studies ISSN 2028-9324 Vol. 17 No. 1 Jul. 2016, pp. 82-93.
2. Alireza Hossein Nezhad and Mostafa Valizadeh Ardalan. A new approach for the analysis of the nanoparticle's effects on Cu-water nanofluid mixed convection heat transfer and required power in a lid-driven cavity. THERMAL SCIENCE, Year 2016, Vol. 20, No. 2, pp. 405-414.
3. Ahmad Reza Rahmati, Ali Rayat Roknabadi, Mahmoud Abbaszadeh. Numerical simulation of mixed convection heat transfer of nanofluid in a double lid-driven cavity using lattice Boltzmann method. Alexandria Engineering Journal. Volume 55, Issue 4, December 2016, pp. 3101-3114.
4. Elif Büyük Öğüt, Kamil Kahveci. Mixed convection heat transfer of ethylene glycol and water mixture based Al2O3 nanofluids: Effect of thermal conductivity models. Journal of Molecular Liquids 224 (2016) 338–345.

ISSN NO: 2770-4491
Date of Publication:20-08-2022

5. Zhimeng Guo, Jinyu Wang, Aloke K. Mozumder and Prodip K. Das. Mixed Convection of Nanofluids in a Lid-Driven Rough Cavity. Conference Paper · August 2016
6. Mohammad Mastiani, Myeongsub Mike Kim, Ali Nematollah. Density maximum effects on mixed convection in a square lid-driven enclosure filled with Cu-water nanofluids. Advanced Powder Technology 28 (2017) 197–214.
7. [22]Ilhem Zeghbid and Rachid Bessaïh. Mixed Convection in a Lid-Driven Square Cavity With Heat Sources Using Nanofluids. FDMP, vol.13, no.4, pp.251-273, 2017
8. Fatih Selimefendigil, Hakan F. Öztopb, Ali J. Chamkha. Analysis of mixed convection of nanofluid in a 3D lid-driven trapezoidal cavity with flexible side surfaces and inner cylinder. International Communications in Heat and Mass Transfer 87 (2017) 40–51
9. Bijan Karbasifar a, Mohammad Akbari, Davood Toghraie. Mixed convection of Water-Aluminum oxide nanofluid in an inclined lid-driven cavity containing a hot elliptical centric cylinder. International Journal of Heat and Mass Transfer 116 (2018) 1237–1249.
10. M. Jahirul Haque Munshi, Nusrat Jahan, Golam Mostafa. Mixed Convection Heat Transfer of Nanofluid in a Lid-Driven Porous Medium Square Enclosure with Pairs of Heat Source-Sinks. American Journal of Engineering Research (AJER), Volume-8, Issue-6, pp-59-70, 2019.
11. Ishrat Zahan, R. Nasrin and M. A. Alim. Mixed convective hybrid nanofluid flow in lid-driven undulated cavity: Effect of MHD and Joule heating. *Journal of Naval Architecture and Marine Engineering, 16(2019) 109-126.*
12. M.S. Rahman, R. Nasrin and M.I. Hoque. Heat-Mass Transfer of Nanofluid in Lid-Driven Enclosure under three Convective Modes. January 2019, GANIT Journal of Bangladesh Mathematical Society 38:73-83 DOI: 10.3329/ganit.v38i0.39787
13. Md Shajedul Hoque Thakur, Mahmudul Islam, Abrar Ul Karim, Sumon Saha and Mohammad Nasim Hasan. Numerical Study of Laminar Mixed Convection in a Cu-Water Nanofluid Filled Lid-Driven Square Cavity with an Isothermally Heated Cylinder. Cite as: AIP Conference Proceedings 2121, 070017 (2019); https://doi.org/10.1063/1.5115924. Published Online: 18 July 2019
14. Neşe Kekl Ġkcgoglu Çakmak, Hasan H. Durmazucar, Kerim Yapici. A numerical study of mixed convection heat transfer in a lid-driven cavity using Al_2O_3-water nanofluid. International Journal of Chemistry and Technology. Int. J. Chem. Technol. 2020, 4 (1), 22-37.
15. Mostafa Valizadeh Ardalan, Rasool Alizadeh, Abolfazl Fattahi, Navid Adelian Rasi, Mohammad Hossein Doranehgard, Nader Karimi. Analysis of unsteady mixed convection of Cu–water nanofluid in an oscillatory, lid-driven enclosure using lattice Boltzmann method. Journal of Thermal Analysis and Calorimetry, https://doi.org/10.1007/s10973-020-09789-3, Received: 13 April 2020 / Accepted: 4 May 2020.
16. Abdullah A. A. A. Al-Rashed, Ghanbar Ali Sheikhzadeh, Alireza Aghaei, Farhad Monfared, Amin Shahsavar, Masoud Afrand. Effect of a porous medium on flow and mixed convection heat transfer of nanofluids with variable properties in a trapezoidal enclosure. Journal of Thermal Analysis and Calorimetry (2020) 139:741–754.
17. M. A. Waheed, G. A. Odewole and S. O. Alagbe. Mixed convective heat transfer in rectangular enclosures filled with porous medium. ARPN Journal of Engineering and Applied Sciences, VOL. 6, NO. 8, AUGUST 2011.
18. Wael M. El-Maghlany, Mohamed A. Teamah and Ahmed A. Hanafy Enhancement of Mixed Convection Heat Transfer in a Lid-Driven Square Cavity Completely Filled with Porous Material by Sidewalls Sinusoidal Heating. International Review of Applied Engineering Research. ISSN 2248-9967 Volume 2, Number 1 (2012), pp. 55-84.
19. Abdalla M. AlAmiri. Implications of placing a porous block in a mixed-convection heat-transfer, lid-driven cavity heated from below. Journal of Porous Media, 16 (4): 367–380 (2013).
20. Anirban Chattopadhyay, Sreejata Sensarma and Swapan K Pandit. Numerical Simulations of Mixed Convection in a Porous Double Lid Driven Cavity. An International Conference on Mathematical Modeling And Computer Simulation with Applications, IIT Kanpur, December 31, 2013-January 2, 2014.

ISSN NO: 2770-4491
Date of Publication:20-08-2022

21. Satyajit Mojumder, Sourav Saha, M. Rizwanur Rahman, M.M. Rahman, Khan Md. Rabbi, Talaat A. Ibrahim. Numerical study on mixed convection heat transfer in a porous L-shaped cavity. Engineering Science and Technology, an International Journal 20(1) August 2016. DOI: 10.1016/j.jestch.2016.07.005
22. Ahmad Ababaei, Mahmoud Abbaszadeh, Ali Arefmanesha and Ali J. Chamkh. Numerical simulation of double-diffusive mixed convection and entropy generation in a lid-driven trapezoidal enclosure with a heat source. NUMERICAL HEAT TRANSFER, PART A https://doi.org/10.1080/10407782.2018.1459139. pp. 1-20, 2018.
23. Salma Parvin and Rehena Nasrin. Magnetohydrodynamic Mixed Convection Heat Transfer in a Lid-driven Cavity with Sinusoidal Wavy Bottom Surface. Journal Tri. Math.Soci.12(2010) 1-9.
24. Khaled Al-Salem, Hakan F. Oztop, Ioan Pop, and Yasin Varol. Effects of moving lid direction on MHD mixed convection in a linearly heated cavity. International Journal of Heat and Mass Transfer 55 (2012) pp. 1103–1112.
25. Ziafat Mehmood and Tabish Javed. MHD-Mixed convection flow in a lid driven trapezoidal cavity under uniformly/ non-uniformly heated bottom wall. International Journal of Numerical Methods for Heat and Fluid Flow · May 2016 DOI: 10.1108/HFF-01-2016-0029.
26. N. A. Bakar, A. Karimipour, and R. Roslan. Effect of Magnetic Field on Mixed Convection Heat Transfer in a Lid-Driven Square Cavity. Journal of Thermodynamics, Accepted 14 February 2016.
27. M. Borhan Uddin, M. M. Rahman, M. A. H. Khan, R. Saidur, Talaat A. Ibrahim. Hydromagnetic double-diffusive mixed convection in trapezoidal enclosure due to uniform and nonuniform heating at the bottom side: Effect of Lewis number. Alexandria Engineering Journal (2016) 55, 1165–1176.
28. M. Rashad, Sameh E. Ahmed, Waqar A. Khan, and M. A. Mansour. Inclined MHD Mixed Convection and Partial Slip of Nanofluid in a Porous Lid-Driven Cavity with Heat Source-Sink: Effect of Uniform and Non-Uniform Bottom Heating. Journal of Nanofluids, Vol. 6, pp. 1–11, 2017.
29. Sameh E. Ahmed, Ahmed Kadhim Hussein, M.A. Mansour, Z.A. Raizah, & Xiaohui Zhang. MHD mixed convection in trapezoidal enclosure filled with micropolar nanofluids. Nanoscience and Technology: An International Journal 9(4):343–372 (2018).
30. GH.R. Kefayati, H. Tang. MHD mixed convection of viscoplastic fluids in different aspect ratios of a lid-driven cavity using LBM. International Journal of Heat and Mass Transfer 124 (2018) 344–367.
31. M. Humaun Kabir, M. Jahirul Haque Munshi, Nazma Parveen. Numerical Study of MHD Mixed Convection Heat Transfer of Nanofluid in a Lid-driven Porous Rectangular Cavity with Three Square Heating Blocks. AIP Conference Proceedings 2121, 070002 (2019); https://doi.org/10.1063/1.5115909.
32. Md. Fayz-Al-Asada, M. A. Hossain, M. M. A. Sarker. Numerical Investigation of MHD Mixed Convection Heat Transfer Having Vertical Fin in a Lid-Driven Square Cavity. Cite as: AIP Conference Proceedings 2121, 030023 (2019); https://doi.org/10.1063/1.5115868, Published Online: 18 July 2019.
33. Priyajit Monda, Tapas Ray Mahapatra. Minimization of entropy generation due to MHD double diffusive mixed convection in a lid driven trapezoidal cavity with various aspect ratios. Nonlinear Analysis: Modelling and Control, Vol. 25, No. 4, 545–563, 2020.
34. Abdelkader Boutra, Karim Raguia and Youb Khaled Benkahla. Numerical study of mixed convection heat transfer in a lid-driven cavity filled with a nanofluid. Mechanics & Industry 16, 505 (2015).
35. Z. Said, H.A. Mohammed, R. Saidur. Mixed convection heat transfer of nanofluids in a lid-driven square cavity: A parametric study. International Journal of Mechanical and Materials Engineering (IJMME), Vol. 8 (2013), No. 1, Pages: 48-57.
36. Khanafer, K., & Aithal, S. M. (2013). Laminar mixed convection flow and heat transfer characteristics in a lid driven cavity with a circular cylinder. *International Journal of Heat and Mass Transfer*, *66*, 200-209.